ORNL/CP-101058

EFFECTS OF PLATINUM ADDITIONS AND SULFUR IMPURITIES ON THE MICROSTRUCTURE AND SCALE ADHESION BEHAVIOR OF SINGLE-PHASE CVD ALUMINIDE BOND COATINGS

J.A. Haynes,[1] Y. Zhang,[1] W.Y. Lee,[3] B.A. Pint,[1] I.G. Wright,[1] and K.M. Cooley[1]

[1]Oak Ridge National Laboratory, Oak Ridge, TN 37831-6063
[2]The University of Tennessee, Knoxville, TN 37996-2200
[3]Stevens Institute of Technology, Hoboken, NJ 07030

Abstract

The adhesion of alumina scales to aluminide bond coats is a life-limiting factor for some advanced thermal barrier coating systems. This study investigated the effects of aluminide bond coat sulfur and platinum contents on alumina scale adhesion and coating microstructural evolution during isothermal and cyclic oxidation testing at 1150°C. Low-sulfur NiAl and NiPtAl bond coats were fabricated by chemical vapor deposition (CVD). Lowering the sulfur contents of CVD NiAl bond coatings significantly improved scale adhesion, but localized scale spallation eventually initiated along coating grain boundaries. Further improvements in scale adhesion were obtained with Pt additions. The observed influences of Pt additions included: (1) mitigation of the detrimental effects of high sulfur levels, (2) drastic reductions in void growth along the scale-metal interface, (3) alteration of the oxide-metal interface morphology, and (4) elimination of Ta-rich oxides in the Al_2O_3 scales during thermal cycling. The results of this study also suggested that the microstructure (especially the grain size) of CVD aluminide bond coatings plays a significant role in scale adhesion.

For publication in
Elevated Temperature Coatings: Science and Technology III
Ed. J.M. Hampikian (TMS, Warrendale, PA, 1998).

Research sponsored by the U.S. Department of Energy, Assistant Secretary for Energy Efficiency and Renewable Energy, Office of Industrial Technologies, Advanced Turbine Systems Materials Program, under contract DE-AC05-96OR22464 with Lockheed Martin Energy Research Corporation.

DISCLAIMER

Introduction

Thermal barrier coating (TBC) systems, which are used to protect superalloy components in the hot section of gas turbine engines, typically consist of an oxidation-resistant metallic bond coating overlaid with a thermally insulating ceramic top coating. Aluminide coatings (NiAl or NiPtAl) are commonly used as bond coatings for TBC systems that utilize electron-beam physical vapor deposition (EB-PVD) ceramic top coats [1]. The oxidation resistance of these intermetallic bond coat systems is based on their ability to form a protective, external Al_2O_3 scale. In TBC applications, the Al_2O_3 scale forms along the bond coat-top coat interface and apparently provides a chemical bond between the ceramic top coat and the metallic bond coat. The thermomechanical stability of the interfacial Al_2O_3 scale is the factor that most often limits the durability of current EB-PVD TBC systems [1-3].

Fracture and/or delamination of brittle Al_2O_3 scales occurs when residual stresses due to metal-ceramic thermal expansion mismatches exceed the oxide-metal bond strength. The thermomechanical stability of oxide scales can be influenced by a variety of phenomena, including scale thickness, scale growth stresses [4], void formation along the oxide-metal interface [5], and geometric stresses induced by non-planar surfaces [6]. Oxidation-resistant coatings were originally designed to continuously re-form Al_2O_3 scales once spallation initiated. However, for EB-PVD TBC applications, adhesion of the virgin Al_2O_3 scale is of paramount importance, since significant scale delamination results in concomitant spallation of the ceramic top coat [1,2]. Thus, development of advanced TBC systems requires design of improved bond coatings that form virgin Al_2O_3 scales with optimized adhesion and minimized growth rates.

It is generally agreed that scale adhesion is degraded by segregation of sulfur impurities to the oxide-metal interface [7-9]. Improvements in Al_2O_3 scale and TBC adhesion after de-sulfurization of Ni-based alloys have been documented [8,10,11]. Scale adhesion can also be improved by doping the alloy with proper levels of a reactive element (RE), which alters the oxide scale microstructure and apparently neutralizes detrimental sulfur effects [5,7,12]. However, current fabrication technologies are not capable of uniformly incorporating controlled levels of REs (e.g., Y, Hf, or Zr) into aluminide coatings. Thus, sulfur continues to be a concern, especially with respect to the long-term scale adhesion performance of aluminide bond coatings.

Alloying with Pt is another established method of enhancing scale adhesion. However, the role of Pt in improving scale adhesion is not well understood. A number of Pt-related mechanisms have been proposed, including: mechanical keying of the scale [13], rapid self-healing of Al_2O_3 [14], modification of aluminide Al content [15], inhibition of refractory element diffusion [16], and suppression of void formation along the oxide-metal interface [17,18]. The objective of this paper is to summarize our recent investigations of the effects of S and Pt on the microstructural evolution and scale adhesion behavior of low-sulfur, single-phase chemical vapor deposition (CVD) NiAl and (Ni,Pt)Al bond coatings during isothermal and cyclic oxidation.

Experimental

An yttrium-free version of a second-generation, single-crystal, Ni-based superalloy (René N5') was used as the standard substrate material in this study (Table I). The bulk sulfur content of the low-sulfur (LS) superalloy (which was melt-desulfurized) was ~0.4 ppmw, as measured by glow-discharge mass spectroscopy (GDMS). Coatings were also deposited on a high sulfur (HS) version of the same superalloy (with ~3 ppmw sulfur). All substrate coupons (1.8 cm x 1.4 cm x 0.15 cm) were polished on all surfaces (to 0.05 μm alumina), followed by ultrasonic cleaning.

Low-sulfur NiAl coatings were fabricated on the substrates by a conventional, low Al-activity CVD aluminizing procedure (1100°C for 6-h) [19] that had been modified in order to minimize sulfur contamination [11]. The (Ni,Pt)Al coatings were synthesized by electroplating substrates with ~7 μm Pt and then aluminizing by identical CVD procedures [18,20].

Table I. Composition of Single-Crystal René N5' Substrates

Element	Ni	Co	Cr	Ta	Al	W	Re	Mo	Hf	Ti	C
wt%	63.38	7.33	7.03	6.42	6.05	5.13	3.05	1.40	0.15	0.01	0.05
at%	64.92	7.48	8.13	2.13	13.48	1.68	0.99	0.88	0.05	0.01	0.25

Selected as-deposited NiAl- and (Ni,Pt)Al-coated specimens on LS and HS substrates were tested in an automated cyclic oxidation furnace. Each cycle consisted of a 1-h exposure at 1150°C in dry flowing O_2, followed by a 10-min cooling period in ambient air. Specimens were weighed and inspected after every 20 or 50 cycles. Other NiAl- and NiPtAl-coated specimens, on LS substrates only, were evaluated in isothermal oxidation testing at 1150°C in O_2 flowing at 100 cm^3min^{-1} (using a Cahn model 1000 microbalance). The phase contents of the Al_2O_3 scales and the as-deposited and oxidized coatings were determined by X-ray diffraction (XRD). Surfaces and cross-sections of the coatings and their oxide scales were examined by field-emission gun-scanning electron microscopy (FEG-SEM).

Results and Discussion

Coating Microstructures and Sulfur Impurity Levels

As described previously [11,18-20], the low activity CVD process results in outward-growing layers of columnar-grained, single-phase β-NiAl or β-(Ni,Pt)Al, with an underlying interdiffusion zone consisting of a β matrix with elongated precipitates rich in refractory metals [Fig. 1(a)]. The NiAl and (Ni,Pt)Al coatings were similar in microstructure, with grain diameters ranging from 50 - 120 μm. The average thickness of the NiAl and (Ni,Pt)Al β-phase outer layers (measured from the substrate surface) were 25 and 40 μm, respectively. Coating surfaces were generally flat, with networks of prominent grain boundary surface ridges [Figs. 1(a) and (b)].

Previous work measured the β-phase sulfur level (by GDMS) of the as-deposited CVD NiAl on LS substrates to be less than 0.5 ppmw [11]. Subsequent studies determined that the outer layer of the as-deposited (Ni,Pt)Al coatings on LS substrates contained less than 0.5 ppmw sulfur, with a peak of ~3 ppmw near the coating surface [18,20]. More significantly, the sulfur content in the (Ni,Pt)Al coatings increased to ~140 ppmw at the depth which coincided with the location of the original Pt layer. This increase was due to sulfur contamination of Pt during electroplating.

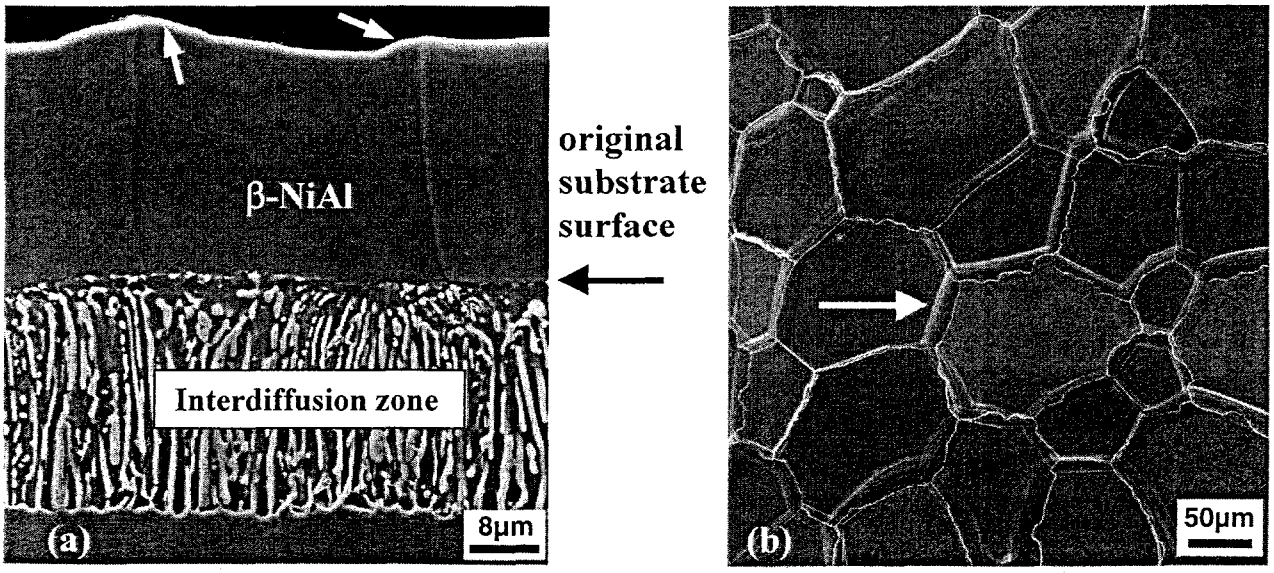

Figure 1. SEM images of: (a) an etched cross-section of an as-deposited, low-sulfur NiAl coating, showing the single-phase β layer with a columnar grain structure, the interdiffusion zone and the morphology of the grain boundary ridges (white arrows); and (b) an as-deposited (Ni,Pt)Al coating surface, showing the network of prominent grain boundary ridges (arrow).

Cyclic Oxidation Behavior

The detrimental influence of sulfur on Al_2O_3 scale adhesion to CVD NiAl coatings during thermal cycle testing at 1150°C was obvious (Fig. 2). Scale adhesion to CVD NiAl coatings on the LS René N5' substrates was significantly improved after reducing the sulfur levels of the coating to less than 1 ppmw [11]. Minor weight losses were measured after 200 1-h cycles of CVD NiAl on LS substrates (Fig. 2). SEM analysis of the NiAl coating surfaces after 200 cycles showed localized scale spallation along the aluminide grain boundary ridges, while scales on the grain surfaces were generally still adherent. By comparison, when identical CVD NiAl coatings were deposited on HS substrates, severe weight losses (indicating massive scale spallation) were measured after only 40 1-h cycles (Fig. 2) [18]. Extensive scale spallation occurred over both grain surfaces and grain boundaries in the NiAl coating on a HS substrate. These results corroborate previous reports of the deleterious influence of sulfur on the oxidation behavior of Ni-based alloys and TBCs (with aluminide bond coats) without RE additions [7,8,10].

The results of these cyclic oxidation experiments strongly suggested that Pt additions mitigate the detrimental effects of sulfur contaminants (from both Pt electroplating and the bulk substrate). The (Ni,Pt)Al coatings on LS substrates displayed excellent Al_2O_3 scale adhesion, even though their sulfur contents were higher than that of NiAl on LS substrates (due to the Pt sulfur contaminants). No weight losses were measured during 500 1-h cycles of the CVD (Ni,Pt)Al coatings on LS substrates, as shown in Fig. 2. Examination of the surfaces of the (Ni,Pt)Al coatings on LS substrates after 200 cycles (by SEM) revealed adherent Al_2O_3 scales, with no scale spallation from the grain boundary ridges (in contrast to the significant grain boundary spallation on the NiAl coatings on LS substrates) [20]. Comparison of the scale adhesion behavior of CVD NiAl and (Ni,Pt)Al on high sulfur (HS) substrates (Fig. 2) further illustrates the capability of Pt to improve scale adhesion in the presence of high sulfur levels. Minor weight losses were measured after 200 cycles of (Ni,Pt)Al on a HS substrate (Fig. 2), as compared to massive scale spallation before 40 cycles for NiAl on a HS substrate.

Although no Al_2O_3 spallation occurred after 200 cycles, minor amounts of cracking were observed in scales on (Ni,Pt)Al grain boundaries. This result suggested that even though the scales on (Ni,Pt)Al were much more adherent than those on NiAl, the grain boundaries will still be preferred sites for scale failure. This conclusion is supported by observations that Al_2O_3 scale failure occurred over cast NiAl grain boundaries [21] and over bond coat grain boundaries of industrial EB-PVD TBCs with CVD (Ni,Pt)Al bond coats (with nominal S levels) [3].

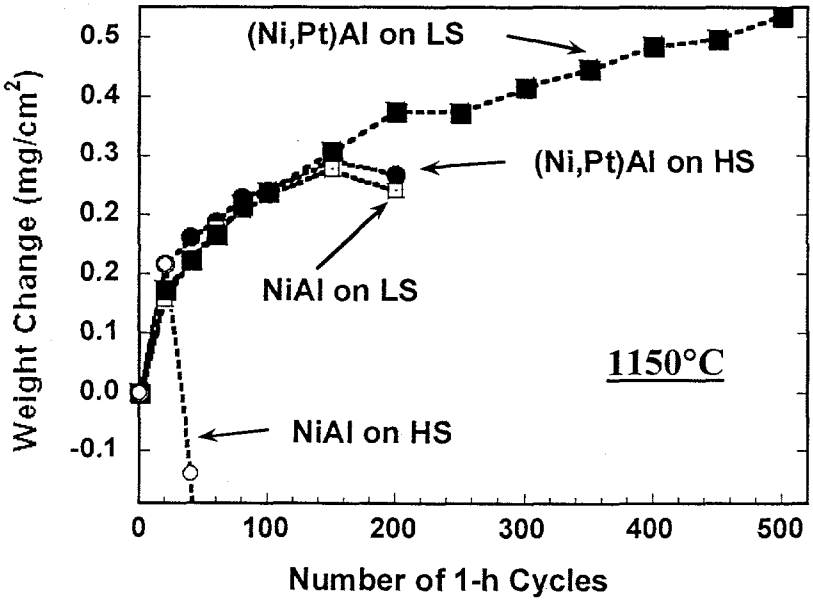

Fig. 2. Representative plots of specimen weight changes during thermal cycle testing at 1150°C.

After 500 cycles of the CVD (Ni,Pt)Al coatings on LS substrates, cracking of grain boundary scales was common, but there was little indication of scale spallation (i.e., no bare metal was exposed). Closer examination of the coating surfaces revealed occasional surface depressions (or valleys) at or near coating grain boundaries. It was concluded that limited amounts of Al_2O_3 spallation did occur between 200 and 500 cycles, but the Al_2O_3 scales re-formed very rapidly on the (Ni,Pt)Al, as has been postulated previously [14]. An alternate (or complementary) explanation of these surface depressions is localized deformation of the coating surface due to oxidation stresses (as will be described in a subsequent section). It should be noted that the beneficial mechanism of accelerated scale re-formation still does not explain the improved initial adhesion of the scales that formed over the grain boundaries, and it does not account for the observed improvements in scale adhesion in the presence of high sulfur levels.

Isothermal Oxidation Behavior

Continuous thermogravimetry of CVD NiAl and CVD (Ni,Pt)Al on LS substrates measured extremely low scale growth rates on both coatings during isothermal oxidation experiments (one specimen of each type was oxidized for 100-h and another for 200-h) [18]. The steady-state oxidation rate of the NiAl coatings (parabolic rate constant, $k_p = 7.0x\ 10^{-14}\ g^2cm^{-4}s^{-1}$) were essentially half that of the (Ni,Pt)Al coatings ($k_p = 1.4x10^{-13}\ g^2cm^{-4}s^{-1}$). By comparison, the isothermal oxidation rates of cast NiAl + Hf ($k_p = 3.8x10^{-13}\ g^2cm^{-4}s^{-1}$) and uncoated LS René N5' ($k_p = 9.6x10^{-13}\ g^2cm^{-4}s^{-1}$) were measurably higher. The average scale thickness on the NiAl and (Ni,Pt)Al coatings was approximately 1.4 μm and 1.95 μm, respectively, after 200-h. These comparisons clearly showed that Pt did not improve scale adhesion by reducing scale growth rates, as has been suggested previously for high activity aluminide coatings [15]. Additions of Hf to cast NiAl can significantly lower scale growth rates [10,12]. Since the oxidation rates of the NiAl coatings were lower than that of cast NiAl+Hf, it is possible that the combination of Hf diffusion from the superalloy and the large coating grains might contribute to the extremely low scale growth rates. Segregation of Hf to the scale or oxide-metal interface is currently being evaluated by transmission electron microscopy. However, it is not anticipated that there is a significant RE effect in this system due to the very low concentration of Hf in the superalloy (0.05 at%) and the poor scale adhesion during cyclic oxidation of CVD NiAl on HS substrates.

Void Growth at Oxide-Metal Interfaces

The most obvious Pt-related difference in coating isothermal oxidation behavior was a drastic reduction in void (or cavity) growth at the oxide-metal interface in the (Ni,Pt)Al coatings, especially along coating grain boundaries [20]. No scale spallation was observed on the (Ni,Pt)Al coating surfaces after 200-h isothermal oxidation, as shown in Fig. 3(a). Comparatively, the scales on low-sulfur CVD NiAl grain surfaces were also adherent, but localized Al_2O_3 spallation occurred along many of the grain boundary ridges after 100 and 200-h isothermal oxidation. Scale spallation from the NiAl grain boundaries revealed numerous large voids in the exposed metal surfaces [Fig. 3(b)]. These voids had the appearance of elongated craters with smooth cavity surfaces, while surrounding metal surfaces contained numerous Al_2O_3 grain imprints [5,22]. Voids were also visible in metallographic cross-sections (by SEM), which allowed analysis of void depths and determinations of whether voids were present beneath scales that had not spalled. Figures 4(a) – (d) show cross-sections of low-sulfur NiAl coatings with grain boundary voids in the β-phase outer layer. Figure 4(a) shows a typical void after 100-h and Fig. 4(b) demonstrates the significant increases in void depth after 200-h. After 200-h, voids were occasionally observed on NiAl grain surfaces (i.e., areas not associated with grain boundaries).

The oxide scales on some NiAl coating grain boundary surfaces appeared intact or only slightly cracked after isothermal oxidation, but examination of cross-sections revealed large voids beneath some of these adherent scales [Fig. 4(c)]. The large cavities underlying these buckled scales were not oxidized, indicating that cracks such as that in Fig. 4(c) occurred during cooling. Comparison of localized scale thickness in Fig. 4(c) also indicates that scale growth was not arrested by the formation of an underlying void. Many grain boundary ridges still contained intact scales, with no evidence of void formation in cross-section. In other areas the NiAl coatings were free of grain boundary voids, but localized regions of the coating surface had experienced significant plastic deformation during the 200-h isothermal exposure [Fig. 5(a)]. Scales were often still adherent on these deformed surfaces. High densities of grain boundary voids were observed in some locations, as illustrated by the cross-section of Fig. 4(d), which shows two voids over adjacent grain boundaries. In contrast, no voids were observed by SEM analysis of (Ni,Pt)Al cross-sections after 100 and 200-h isothermal exposure, indicating that Pt eliminated or significantly altered void growth behavior on these aluminide coatings. Similar reductions in void growth have been observed on cast NiPtAl alloys [10].

Few voids were observed on NiAl surfaces exposed by scale spallation after thermal cycling, as compared to isothermal oxidation. Furthermore, no large voids [such as those in Fig. 4(a) or 4(b)] were observed in coating cross-sections after thermal cycling. The coating microstructures after 200 cycles suggested that voids had formed during the early stages of cyclic oxidation, followed by scale spallation, which left small void cavities (with a concave morphology) above the grain boundaries [similar to that in Fig. 4(a)]. These void cavities oxidized during subsequent cycles. The oxide scales on these grain boundary surfaces often contained evidence of having experienced multiple scale spallation and re-growth cycles. When comparing void formation during isothermal and cyclic oxidation, it should also be noted after 200 1-h cycles almost all of the NiAl grain boundaries had transformed from the Al-rich β-(NiAl) phase to the γ' (Ni_3Al) phase, due to loss of Al from back diffusion into the substrate and consumption of Al to re-grow Al_2O_3 [Fig. 5(b) and Fig. 6(b)]. In contrast, there was no visible γ' presence at the NiAl coating grain boundaries after 200-h isothermal oxidation.

No evidence of void formation or scale spallation was observed in (Ni,Pt)Al cross-sections after 200 cycles or on (Ni,Pt)Al surfaces after 500 cycles. The 500-cycle (Ni,Pt)Al coating specimens are currently undergoing additional cyclic oxidation testing in order to determine their ultimate spallation lifetime. It was concluded that Pt additions drastically reduced the rate of void growth in these aluminide coatings, especially during isothermal oxidation. However, from the SEM analysis it was not clear whether Pt additions also suppressed void nucleation [5].

It was obvious that the drastic reduction in void growth rates was one of the primary reasons for the improved scale adhesion behavior of the Pt-containing coatings (although there may be more than one mechanism by which Pt additions benefit scale adhesion). This effect is even more striking when the high levels of sulfur contaminants in the electroplated Pt are considered. However, the mechanism by which void growth behavior was altered in the Pt-containing coatings was not identified. Doping of aluminides with small concentrations of REs also reduces void formation in the presence of high sulfur levels (by preferential segregation to the oxide-metal interface or by forming stable RE-sulfides), but previous work on cast NiAl and NiPtAl has indicated that Pt does not behave as a RE [10,17]. Thus, while is it clear that the addition of Pt can mitigate sulfur effects, at least during short-term exposures, it is likely that this effect is not due to a Pt-sulfur reaction.

It is possible that the Pt effect is diffusion related, since rapid void growth over NiAl coating grain boundaries (which are rapid diffusion paths) was eliminated in the presence of Pt additions during short-term isothermal exposures. It has previously been reported that Pt additions to cast NiAl only postponed void growth and scale failure, as compared to the longer-term beneficial effects of doping with Hf [10,17]. These observations suggests two possibilities. The first is that Pt retards some diffusion-controlled mechanism (such as sulfur segregation) that is ultimately

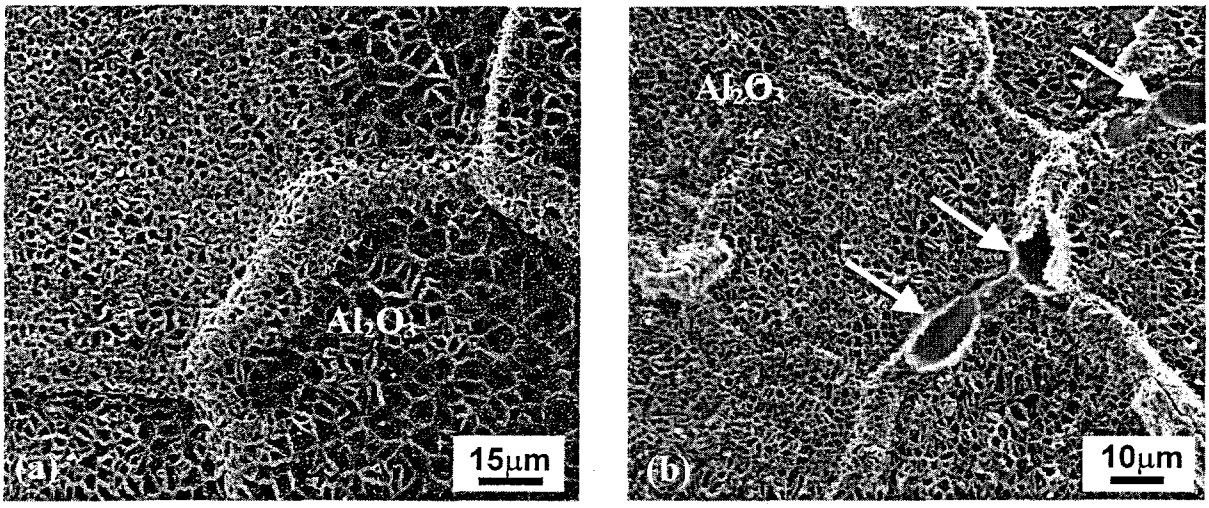

Fig. 3. SEM images of coating surfaces after 200-h isothermal oxidation, showing: (a) adherent Al_2O_3 scales on (Ni,Pt)Al surfaces and grain boundary ridges; and (b) grain boundary voids (arrows) and localized Al_2O_3 scale spallation along the grain boundaries of the low-S NiAl coating.

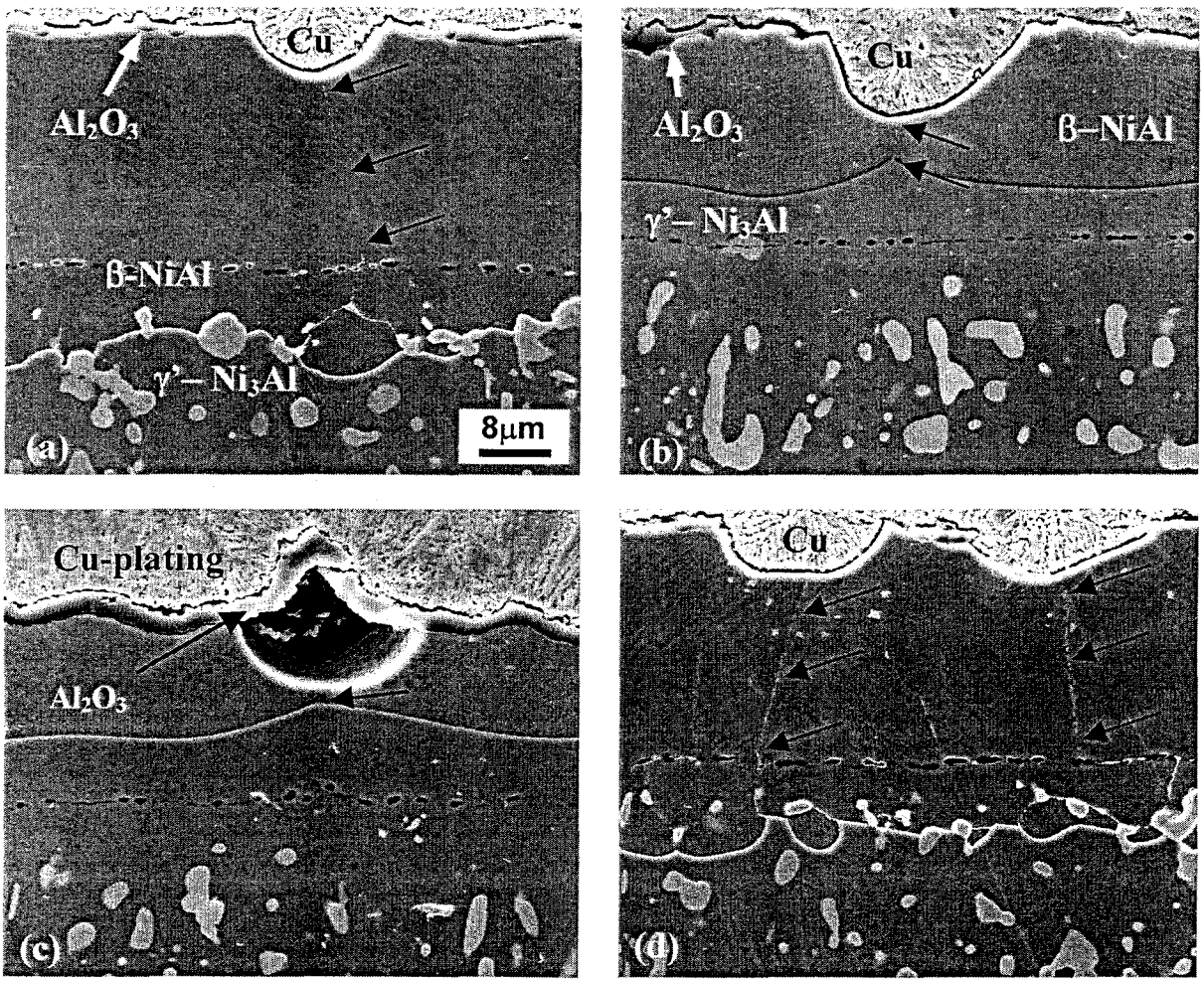

Fig. 4. SEM images of voids on columnar β-NiAl grain boundaries (black arrows) of low-S CVD NiAl coating cross-sections after isothermal oxidation at 1150°C: (a) typical void after 100-h; (b) void depth increased after 200-h; (c) void with overlying, buckled scale after 200-h; (d) voids on adjacent grain boundaries after 100-h. Scales that remained on the surfaces of (a), (b) and (d) are faintly visible due to charging. Void cavity surfaces were not oxidized, indicating the scales over the grain boundary voids remained intact (c) and crack-free at temperature (and spalled or cracked on cooling). The interdiffusion zone matrix transformed to γ'-Ni_3Al as the β-phase was depleted.

responsible for void growth and scale spallation. A second possibility is that the metal-oxide interface in (Ni,Pt)Al is much stronger than the simple aluminide so that spallation occurs at increased scale thickness; this argument implies that a RE-doped aluminide has an even stronger oxide-metal bond. It has been suggested elsewhere that void nucleation may be reduced or postponed by a higher-strength interface [5,10].

Coating Compositions and β-Phase Depletion

Consumption of Al (by Al_2O_3 formation and interdiffusion) eventually leads to depletion of the Al-rich β-(NiAl) phase, which can be a precursor to a loss of protective capacity in many oxidation-resistant coating systems. There were moderate amounts of uniform depletion of the β-phase in the (Ni,Pt)Al coatings after 200-h and 200 1-h cycles [Fig. 6(a)], whereas β-phase depletion in the thinner NiAl coatings was more severe and generally less uniform [Figs. 4(a-d) and Fig. 6(b)].

The near-surface regions of both the NiAl and NiPtAl coatings still consisted of a continuous layer of β phase after 200-h isothermal oxidation, as shown in Figs. 4(a) – (d) and Fig. 5(a). In order to compare the diffusion behavior of various elements in the simple aluminide and the Pt-containing aluminide coatings, bulk compositional profiles (by electron microprobe analysis) were measured across the cross-sections of the β-phase outer layers in the NiAl and (Ni,Pt)Al coatings (in the as-deposited condition and after 100-h and 200-h isothermal oxidation). No significant differences in the bulk concentrations of refractory metal elements (i.e., W, Ta, Re, Mo) in the β-phase were detected as a result of Pt incorporation. In fact, submicron-sized particles rich in refractory-metal elements were observed along the columnar grain boundaries of both the NiAl and (Ni,Pt)Al coatings before and after oxidation. There were slight reductions in Ni, Cr and Co in the β-phase of the (Ni,Pt)Al (due to Pt incorporation). Although there was a slightly higher Al content in the near-surface region of the as-deposited (Ni,Pt)Al, the Al content of the β-phase region of both coatings was homogeneous after isothermal oxidation. The average Al concentration in the β-phase surface region was ~39 atomic percent for both coatings in the as-deposited condition. The Al content in both NiAl and (Ni,Pt)Al decreased to a constant value of ~32 atomic percent after 100 and 200-h isothermal oxidation. Thus, the observed improvements in scale adhesion in the presence of a Pt addition could not be related to an increased atomic percentage of Al in the coating β-phase [15] or prevention or significant reduction of refractory metal diffusion in the bulk coating [16].

The phase distribution within the NiAl coating after 200 1-h cycles was significantly different than after 200-h isothermal oxidation. As shown in the back scattered electron image of Fig. 6(b) and the secondary electron image of Fig. 5(b), there was significant localized depletion of the β-phase (darker-contrast phase) surrounding the columnar NiAl grain boundaries and at some near-surface regions. The lighter-contrast phases in the outer layer have transformed to γ'. The small, near-surface pockets of γ' in Fig. 6(b) are regions where scale spallation and re-formation occurred. The surfaces above these areas were often slightly concave [Fig. 5(b) and Fig. 6(b)], possibly due to void formation and scale spallation, as discussed previously. Localized transformation to γ' after 200 cycles was due to Al depletion (by oxidation and substrate interdiffusion). The rate of grain boundary β-depletion was more rapid during cyclic oxidation because scale spallation occurred from the grain boundaries, resulting in consumption of additional Al during re-formation of Al_2O_3. However, the reduction in thickness of the β-phase of the bulk coating grains appeared to be lower after cyclic oxidation, as can be seen by comparison of Figs. 5(a) and (b). As can also be seen by comparison of Fig. 1(a) to Figs. 4(a-d) and Figs. 5(a) and (b), significant coarsening of the bright-contrast refractory metal precipitates in the interdiffusion zone was observed after isothermal oxidation, whereas particle coarsening was less obvious after cyclic oxidation testing. It is not clear whether the difference in refractory-metal particle size and distribution resulted in differences in interdiffusion behavior, although there were some indications that localized β-phase depletion rates could be reduced by the presence of these particles (as will be discussed below).

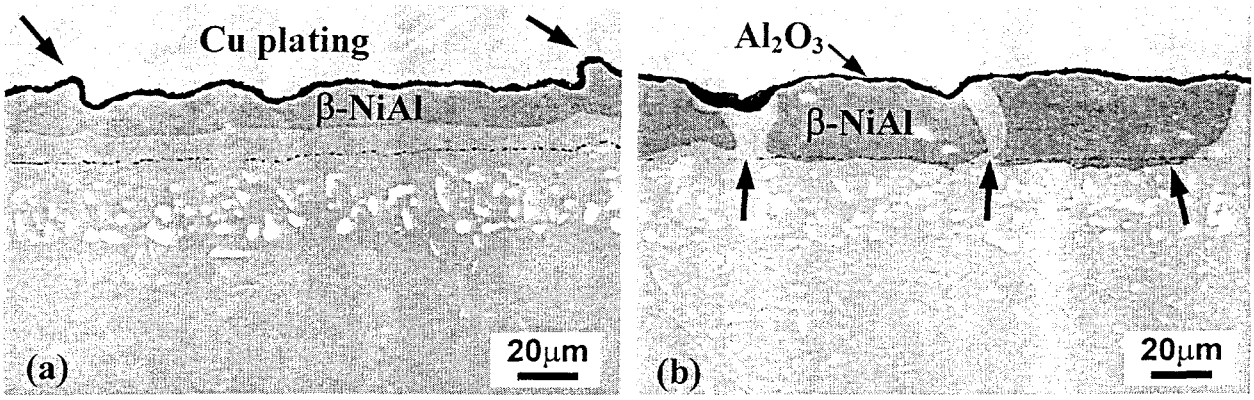

Fig. 5. Secondary electron images of low-S NiAl coating cross-sections, showing: (a) adherent scales on locally deformed coating surfaces (arrows) after 200-h isothermal oxidation; and (b) oxidized, concave coating surfaces over the brighter-contrast β-depleted grain boundaries (arrows) after 200 1-h cycles. Note the significant differences in refractory particle size and β-phase distribution after similar periods of isothermal and cyclic oxidation.

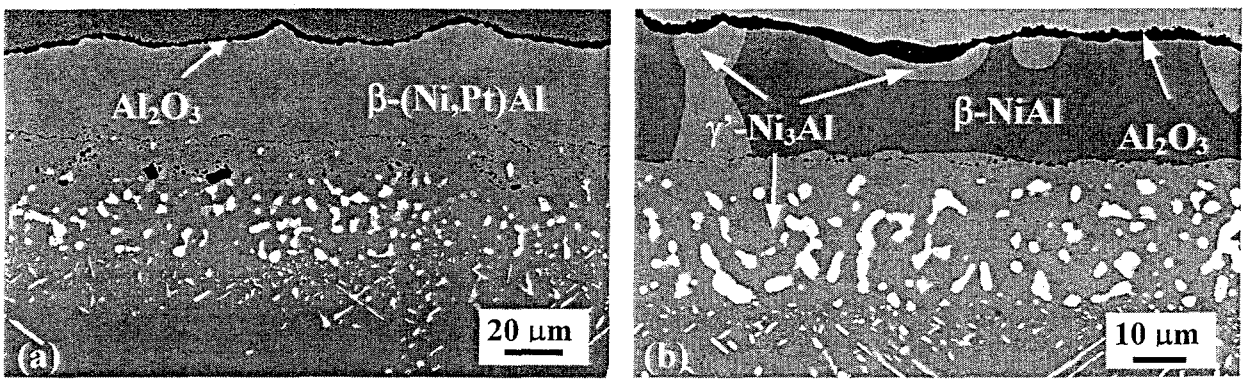

Fig. 6. Back scattered electron images of coating cross-sections after 200 1-h cycles at 1150°C on LS substrates, comparing: (a) (Ni,Pt)Al coating with very little β-depletion in the single-phase region; and (b) β-(NiAl) depletion along the columnar grain boundaries on a NiAl coating. The β-γ' phase contrast in (a) is less obvious due to Pt incorporation.

In general, depletion of the β-phase in the (Ni,Pt)Al after 200 cycles was limited to the interdiffusion zone (although there were a few small near-surface regions that had transformed to a lower-Al phase). No continuous β-depletion was observed along any of the columnar (Ni,Pt)Al grain boundaries after 200 cycles. This improvement in β-phase stability on (Ni,Pt)Al versus NiAl was at least partially due to the superior scale adhesion. It was not clear whether it was also due to an alteration in coating interdiffusion behavior due to the presence of Pt.

Since the solubility of refractory metal elements is greater in γ' than in β [23], a secondary consequence of β depletion at the NiAl grain boundary surfaces was the formation of rapid-growing, less protective oxides. The Al_2O_3 scales immediately over the β-depleted NiAl grain boundaries often contained bright-contrast oxides that were Ta-rich [Fig. 7(a)]. Formation of these oxides diminished the protective capacity of the scales that formed over the grain boundaries, further accelerating the rate of scale spallation. This observation further emphasizes the importance of β-phase stability and coating microstructure in governing the long-term oxidation behavior of aluminide bond coat systems with columnar grain structures.

Another interesting observation was that the rate of localized β-phase depletion in the NiAl coatings was apparently altered by the presence of certain interfacial precipitates rich in refractory metals. The β-phase was depleted well into the single-phase region of the NiAl coating after 200-h. However, as shown in Fig. 7(b), at some locations β depletion appeared to

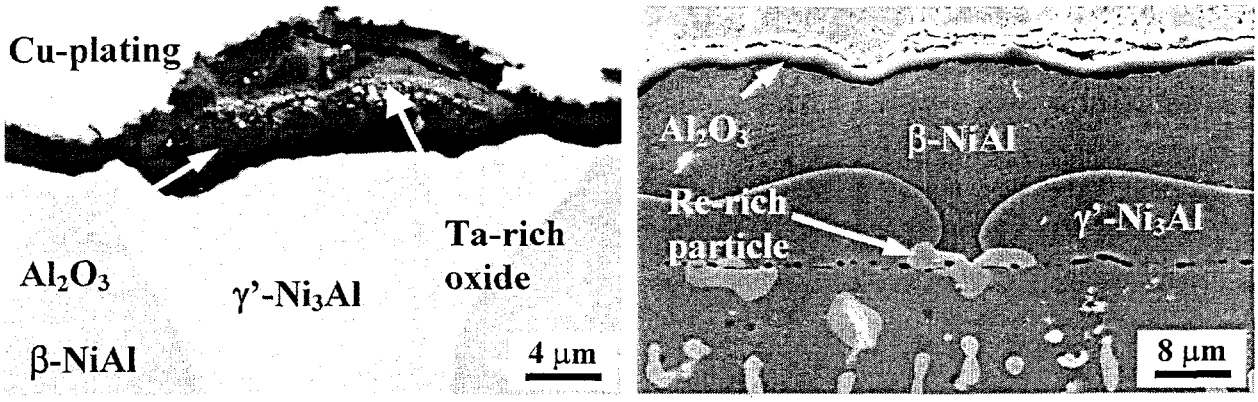

Fig. 7. SEM images of coating cross-sections, showing: (a) bright-contrast Ta-rich oxides within the Al_2O_3 scale over a β-depleted NiAl coating grain boundary after 200 1-h cycles at 1150°C; and (b) an apparent localized reduction in β-phase depletion over a Re-rich particle after 200-h isothermal oxidation of low-sulfur CVD NiAl on a LS substrate.

be significantly reduced in the region immediately above Re-rich particles (the bright-contrast particle) at the coating-substrate interface. Although various types of refractory-rich particles were formed in the interdiffusion zone and along the interface between the coating and the original substrate surface, the particles that appeared to stabilize the β-phase were always enriched in Re. Furthermore, since these results were obtained on isothermal specimens (where the relative rate of β-depletion due to continued growth of the adherent scale was relatively constant), the reduction in β-phase depletion may have been related to inhibition of interdiffusion with the substrate. This effect requires further study.

Oxide Scale Microstructures

The general surface microstructures of the Al_2O_3 scales on NiAl and (Ni,Pt)Al coatings were essentially identical [as shown in Figs. 3(a) and (b)], although there were noticeable differences in the oxide-metal interface morphologies. The oxide scales (which were α-Al_2O_3 by XRD) on all specimens had a wrinkled appearance due to the presence of very fine ridges on the Al_2O_3 surfaces [Figs. 3(a) and (b)]. This ridged microstructure is typical of Al_2O_3 scales that form on aluminides and apparently results from phase transformations during transient oxidation [24]. The density of the resultant Al_2O_3 ridges varied as a function of grain orientation, as indicated by comparison of the adjacent coating grains in Fig. 3(a). The size and geometry of the very fine Al_2O_3 ridges is illustrated in the scale cross-section of Fig. 8(a). No evidence of columnar grain structures (which are an indication of a RE effect) was observed by high magnification FEG-SEM of either fracture cross-sections or metallographic cross-sections of these very thin Al_2O_3 scales. Cross-sections of Al_2O_3 scales on (Ni,Pt)Al coatings revealed small rectangular-shaped metallic protrusions at periodic intervals along the oxide-metal interface [Fig. 8(a)]. By comparison, this type of protrusion morphology was not prevalent along the scale-metal interfaces of the NiAl coatings. Oxide-metal protrusions of this type have been previously reported on cast PtAl alloys, and a mechanism by which Pt-related mechanical keying improves scale adhesion has been proposed [13]. Although it is possible that mechanical keying contributed to the improved scale adhesion on (Ni,Pt)Al coatings, such a mechanism would not readily account for the observed reductions in void formation over coating grain boundaries.

Coating Surface Deformation

Plastic deformation of localized regions of the NiAl and (Ni,Pt)Al coating surfaces appeared to have occurred after both isothermal and cyclic oxidation, as indicated by comparison of the as-deposited coating in Fig. 1(a) with the oxidized coatings in Figs. 5(a), 6(b) and 8(b). It is

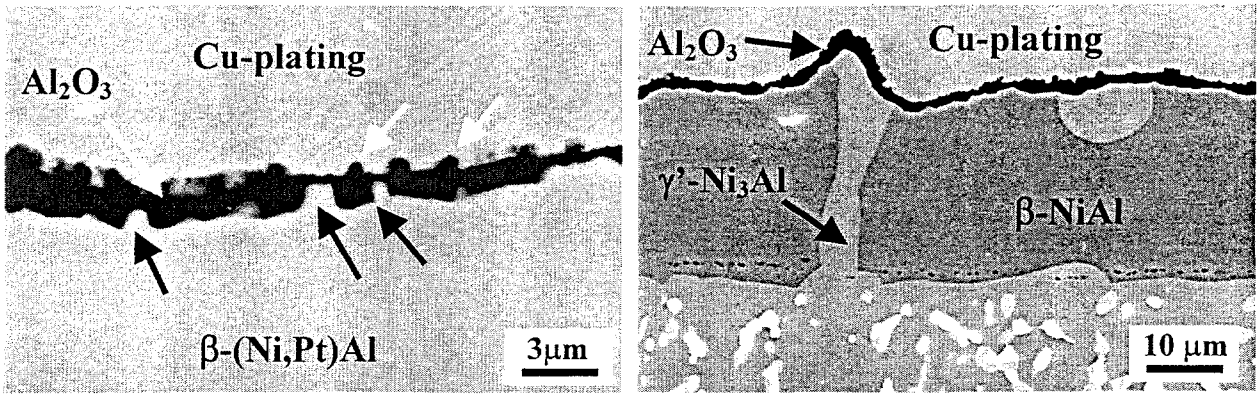

Fig. 8. SEM images of coating cross-sections showing: (a) the scale surface ridges (white arrows) and the metal protrusions (black arrows) in the oxide-metal interface of the Al_2O_3 scale on an (Ni,Pt)Al coating after 100-h isothermal oxidation; and (b) significant deformation of an NiAl coating surface after 200 1-h cycles. Note the β-depleted grain boundary and the adherent Al_2O_3 scale on the sharp peak of the deformed surface.

interesting to note that adherent scales were often observed on the sharp peaks of the deformed coating surfaces (even on NiAl), as shown in Fig. 8(b). It was concluded that there was no effect of Pt to prevent plastic deformation of the coating surface due to oxidation-related stresses, in agreement with previous results [14].

Summary

Significant improvements in Al_2O_3 scale adhesion were demonstrated by reducing sulfur impurities in single-phase CVD aluminide (NiAl) bond coatings on desulfurized, single-crystal superalloys. However, preferential scale spallation eventually occurred along the NiAl coating grain boundaries during cyclic oxidation at 1150°C. Extensive growth of large oxide-metal voids occurred over NiAl grain boundaries during isothermal oxidation. Thus, coating microstructure (especially grain size) plays an important role in determining scale stability. The addition of Pt to low-sulfur CVD aluminide coatings provided significant further improvements in scale adhesion, even though the electroplated Pt also introduced higher levels of sulfur impurities. Platinum additions also significantly improved scale adhesion on superalloys with high sulfur levels, suggesting the Pt additions are capable of mitigating the detrimental effects of sulfur. The most dramatic effect of Pt additions was the elimination of void growth along the oxide-metal interface during short-term isothermal oxidation testing (200-h at 1150°C).

The results of this research suggested that, for the system described in this paper, Pt incorporation did not: (1) decrease the steady-state isothermal growth rate of the Al_2O_3 scale, (2) prevent incorporation of refractory elements into the coating during fabrication, (3) measurably reduce diffusion rates of refractory metal elements into the coatings during oxidation, (4) prevent incorporation of refractory-metal particles along the columnar coating grain boundaries, (5) prevent aluminide coating surface deformation, (6) alter the average β-phase Al concentration.

These results also suggest that there may be multiple beneficial effects associated with the addition of Pt to aluminide bond coatings, including the following: (1) improvements in general oxide scale adhesion during isothermal and cyclic oxidation, (2) reduction or prevention of void growth at the oxide-metal interface (especially at coating grain boundaries) during short-term isothermal exposures, (3) mitigation of detrimental effects of sulfur on scale adhesion (even at relatively high sulfur levels), (4) acceleration of Al_2O_3 scale re-growth after spallation, and (5) prevention or reduction of the formation of Ta-rich secondary oxides after β-depletion.

Acknowledgments

The authors thank C. Kortovich and L. Graham of PCC Airfoils for providing the alloy specimens, B. Warnes and N. DuShane of Howmet Corporation for Pt electroplating, L.D. Chitwood and G. Garner at ORNL for assisting with the oxidation experiments. The authors also thank P. Tortorelli, and M. Lance at ORNL for reviewing the manuscript. Research sponsored by the U.S. Department of Energy, Assistant Secretary for Energy Efficiency and Renewable Energy, Office of Industrial Technologies, Advanced Turbine Systems Materials Program, under contract DE-AC05-96OR22464 with Lockheed Martin Energy Research Corporation.

References

1. P. K. Wright, *Mater. Sci. Eng.*, A245 (1998), 191-200.
2. S.M. Meier, D.M. Nissley, K. D. Sheffler, S. Bose, *J. Eng. Gas Turbine Power*, 112 (1990), 522-527.
3. M. Gell, K. Vaidyanathan, B. Barber, J. Cheng and E. Jordan, "Mechanisms of Spallation in Platinum Aluminide/EB-PVD Thermal Barrier Coatings", submitted to *Metall. Trans. A* (1998).
4. Stott, F. H. and A. Atkinson, *Mater. High Temp.*, 12 (2-3) (1994), 195-207.
5. B.A. Pint, *Oxid. Met.*, 48 (3/4) (1997), 303-328.
6. A. G. Evans, G. B. Crumley and R. E. Demaray, *Oxid. Met.*, 20 (1983), 193-216.
7. J.G. Smeggil, A.W. Funkenbusch, and N.S. Bornstein, *Metall. Trans. A.*, 17A (1986), 923-932.
8. J.L. Smialek, D.T. Jayne, J.C. Schaeffer, W.H. Murphy, *Thin Solid Films*, 253 (1994), 285-292.
9. P.Y. Hou and J. Stringer, *Oxid. Met.*, 38 (5/6) (1992), 323-345.
10. B.A. Pint, I.G. Wright, W.Y. Lee, Y. Zhang, K. Pruβner, and K.B. Alexander, *Mater. Sci. Eng.*, A245 (1998), 201-211.
11. W.Y. Lee, Y. Zhang, I.G. Wright, B.A. Pint, and P.K. Liaw, *Metall. Trans. A*, 29A (1998), 833-841.
12. B.A. Pint, *Oxid. Metal.*, 45 (1996), 1-37.
13. E.J. Felten and F.S. Pettit, *Oxid. Metal*, 10 (3) (1976), 189-223.
14. R. Streiff, O. Cerclier and D.H. Boone, *Surf. Coat. Tech.*, 32 (1987), 111-126.
15. J. Schaeffer, G.M. Kim, G.H. Meier and F.S. Pettit, The Role of Active Elements in the Oxidation Behavior of High Temperature Metals and Alloys, Ed. E. Lang (1988), 231-267.
16. M.R. Jackson and J.R. Rairden, *Metall. Trans. A*, 8A (1977) 1697-1707.
17. E.C. Dickey, B.A. Pint, K.B. Alexander, and I.G. Wright: High Temperature Surface Engineering, J. Nicholls, ed., (Institute of Materials, London, 1998) in press.
18. Y. Zhang, Effects of Sulfur Impurities and Platinum Incorporation on the Oxidation Behavior of Aluminide Coatings Synthesized by Chemical Vapor Deposition (Ph.D. Thesis, The University of Tennessee, 1998).
19. B.M. Warnes and D.C. Punola, *Surf. Coat. Technol.*, 94-95 (1997), 1-6.
20. Y. Zhang, W.Y. Lee, J.A. Haynes, I.G. Wright, B.A. Pint and P.K. Liaw, "Synthesis and Cyclic Oxidation Behavior of a (Ni,Pt)al Coating on a Desulfurized Ni-base Superalloy", submitted to *Metall. Trans. A*, (1998).
21. A. Katsman, H.J. Grabke and L. Levin, *Oxid. Met.*, 46 (3/4) (1996), 313-331.
22. J. L. Smialek, *Metall. Trans.*, 9A (1978), 309.
23. C.C. Jia, K. Ishida and T. Nishizawa, *Metall. Trans. A*, 25A (1994), 473-485.
24. G. C. Rybicki and J.L. Smialek, *Oxid. Met.*, 31 (3/4) (1989), 275-304.